

Spatially explicit predictions of food web structure from regional-level data

Gabriel Dansereau^{1,2} Ceres Barros³ Timothée Poisot^{1,2}

¹ Département de sciences biologiques, Université de Montréal, Montréal, QC, Canada ² Quebec Centre for Biodiversity Science, Montréal, QC, Canada ³ Department of Forest Resources Management, University of British Columbia, Vancouver, BC, Canada

Correspondence to:

Gabriel Dansereau — gabriel.dansereau@umontreal.ca

Abstract: Knowledge about how ecological networks vary across global scales is currently limited given the complexity of acquiring repeated spatial data for species interactions. Yet, recent developments of metawebs highlight efficient ways to first document possible interactions within regional species pools. Downscaling metawebs towards local network predictions is a promising approach to use current data to investigate the variation of networks across space. However, issues remain in how to represent the spatial variability and uncertainty of species interactions, especially for large-scale food webs. Here, we present a probabilistic framework to downscale a metaweb based on the Canadian mammal metaweb and species occurrences from global databases. We investigated how our approach can be used to represent the variability of networks and communities between ecoregions in Canada. Species richness and interactions followed a similar latitudinal gradient across ecoregions but simultaneously identified contrasting diversity hotspots. Network motifs revealed additional areas of variation in network structure compared to species richness and number of links. Our method offers the potential to bring global predictions down to a more actionable local scale, and increases the diversity of ecological networks that can be projected in space.

This work is released by its authors under a CC-BY 4.0 license



Last revision: *July 26, 2024*

1 Introduction

2 Because species interactions vary in time and space, and because species show high turnover over larger spatial
3 extents, adequately capturing the diversity of ecological networks is a challenging task (Jordano 2016). Most
4 studies on food webs have previously focused on local networks limited in size and extent, and are rarely
5 replicated in space or time (Mestre *et al.* 2022). Interactions can show important variations in space (Poisot *et*
6 *al.* 2015; Zarnetske *et al.* 2017), yet available network data also show important geographical bias by focusing
7 sampling efforts in a few areas or biomes, limiting our ability to answer questions in many biomes and over
8 broad spatial extents (Poisot *et al.* 2021). Moreover, global monitoring of biotic interactions is insufficient to
9 properly describe and understand how ecosystems are reacting to global change (Windsor *et al.* 2023).

10 Approaches to predict species interactions (*e.g.*, Desjardins-Proulx *et al.* 2017; Morales-Castilla *et al.* 2015) are
11 increasingly used as an alternative to determine potential interactions; they can handle limited data to
12 circumvent data scarcity (Strydom *et al.* 2021), but are still rarely used to make explicitly spatial predictions.

13 As a result, there have been repeated calls for globally distributed interaction and network data coupled to
14 repeated sampling in time and space (Mestre *et al.* 2022; Windsor *et al.* 2023), which will help understand the
15 macroecological variations of food webs (Baiser *et al.* 2019). Despite these limitations, food web ecologists
16 often can infer a reasonable approximation of the network existing within a region. This representation, called a
17 metaweb, contains all possible interactions between species in a given regional species pool (Dunne 2006), and
18 provides a solid foundation to develop approaches to estimate the structure of networks at finer spatial scales.

19 When assembled by integrating different data sources (and potentially with additional predictive steps), the
20 metaweb allows to overcome sampling limitations and to raise network data to a global scale. For example,
21 Albouy *et al.* (2019) coupled data on fish distributions with a statistical model of trophic interactions to provide
22 estimates of the potential food web structure at the global scale. Recent studies have focused on assembling
23 metawebs for various taxa through literature surveys and expert elicitation (European terrestrial tetrapods,
24 Maiorano *et al.* 2020) or using predictive tools (marine fishes, Albouy *et al.* 2019; Canadian mammals,
25 Strydom *et al.* 2022). At a finer spatial scale, the local food webs (*i.e.*, the local “realization” of the metaweb
26 when combined with species distributions, Poisot *et al.* 2012) reflect local environmental conditions but still
27 retain the signal of the metaweb to which they belong (Saravia *et al.* 2022). Given this, Strydom *et al.* (2023)
28 defended that predicting the metaweb’s structure should be the core goal of predictive network ecology.

29 Assuming there is a strong link between the metaweb and its local realizations, more accurate predictions of the

metaweb will have the potential to bring us closer to producing accurate local (downscaled) predictions (Strydom *et al.* 2023). Therefore, establishing or predicting the metaweb should be the first target in communities where data about local realizations (*i.e.*, documented interactions at specific places) are lacking. Our approach differs from using interactions to improve predictions of species distributions, as has been done by recent studies (Lucas *et al.* 2023; Moens *et al.* 2022; Poggiato *et al.* 2022). Although the two are complementary, and answer long-standing calls to include interactions within species distribution models (Wisz *et al.* 2013), predicting networks in space is a different task serving a different goal: focusing first on the distribution of network structures and its drivers rather than on the distribution of species.

Explicit spatial predictions of the structure of species interaction networks (downscaled metaweb predictions) are essential, as they allow comparisons with extant work for species-rich communities. Recent approaches to metaweb downscaling combined a regional metaweb with species distribution maps to generate local assemblages for European tetrapods (Braga *et al.* 2019; Galiana *et al.* 2021; Gaüzère *et al.* 2022; O'Connor *et al.* 2020), Barents Sea marine taxa (Kortsch *et al.* 2019), and North Sea demersal fishes and benthic epifauna (Frelat *et al.* 2022). These downscaled assemblages open up novel ways to study network structures, such as assessing changes in food web structure across space (Braga *et al.* 2019), or describing the scaling of Network Area Relationships (NARs, Galiana *et al.* 2021). Other examples have shown that the metaweb can be used to investigate large-scale variation in food web structure, indicating high geographical connections and heterogeneous robustness against species extinctions (Albouy *et al.* 2019), which are only apparent when the local and global networks are *both* available. Further comparisons between network structure and other community properties are relevant as they may highlight new and surprising elements regarding network biogeography. For instance, Frelat *et al.* (2022) found a strong spatial coupling between community composition and food web structure, but a temporal mismatch depending on the spatial scale. Poisot *et al.* (2017) found that interaction uniqueness captures more composition variability than community uniqueness, and that sites with exceptional compositions might differ for networks and communities, because species distributions and species interactions had different bioclimatic drivers. Spatialized network data will allow these comparisons, identifying important conservation targets for networks and whether they differ geographically from areas currently prioritized for biodiversity conservation.

Yet, downscaling a regional metaweb towards local network predictions that reflect the spatial variability of interactions remains an important methodological challenge. Even when the metaweb is known, local networks have been shown to vary substantially and differ both amongst themselves and from the metaweb (McLeod *et al.*

2021). This emphasizes the need for methods to generate local, downscaled network predictions. A potential limitation to previous downscaling approaches is that they assumed interactions are equiprobable across space, which ignores well-documented interaction variability, and masks the effect of environmental conditions on interaction realization (Braga *et al.* 2019). As a consequence, this can over-represent interactions locally, but also lead to local predicted networks that are more homogeneous than they should. In contrast, recent studies argued that seeing interactions as probabilistic (rather than binary) events allows us to account for their variability in space (Poisot *et al.* 2016) and that this should also be reflected at the metaweb level (Strydom *et al.* 2023). Gravel *et al.* (2019) introduced a probabilistic framework describing how the metaweb can generate local realizations and showed how it could be used for modelling interaction distributions. This approach to downscaling is especially relevant when combined with *in situ* observations of interactions and local networks to train interaction models. However, such data is rarely available across broad spatial extents (Hortal *et al.* 2015; Poisot *et al.* 2021; Windsor *et al.* 2023). Spatially replicated interaction data required for such models are especially challenging to document with large food web such as European tetrapod and Canadian mammal metawebs (Maiorano *et al.* 2020; Strydom *et al.* 2022), where hundreds of species result in tens of thousands of species pairs that may potentially interact, over continental-scale spatial extents. We currently lack a downscaling framework that is both probabilistic and can be trained without replicated *in situ* interaction data. But the lack of *in situ* interaction data actually constitutes an interesting opportunity: adopting a probabilistic view can allow propagating uncertainty, which can play a key role in evaluating the quality (and expected variability) of the predictions. Assessing model uncertainty would enable us to determine to which degree we should trust our predictions and to identify what to do to improve the current knowledge.

Here, we present a workflow to downscale a metaweb in space, and illustrate it by spatially reconstructing local instances of a probabilistic metaweb of Canadian mammals. We do so using a probabilistic approach to both species distributions and interactions in a system without spatially replicated interaction data. We then explore how the spatial structure of the downscaled metaweb varies in space and how the uncertainty in predicted interactions can be made spatially explicit. We further show that the downscaled metaweb can highlight important biodiversity areas and bring novel ecological insight compared to traditional community measures like species richness or compositional uniqueness. We conclude by listing key considerations for the validation of such predictions.

88 **Methods**

89 In Fig. 1, we present a conceptual overview of the predictive pipeline leading to the downscaled metaweb. Its
90 components were grouped as non-spatial and spatial data, localized site steps (divided into species, species-pair,
91 and network level steps), and the final downscaled, spatialized metaweb. Throughout these steps, we highlight
92 the importance of presenting the uncertainty of interactions and their distribution in space, as well as the
93 variability in the structure of reconstructed networks. We argue that this requires adopting a probabilistic view
94 of both species presence and interactions, and incorporating this variation between scales.

95 [Figure 1 about here.]

96 **Data**

97 **Metaweb**

98 We collected probabilistic interaction data from the reconstructed metaweb of trophic interactions between
99 Canadian mammals from Strydom *et al.* (2022). This metaweb is a-spatial, *i.e.*, it represents interactions
100 between mammals that can occur anywhere in Canada. It contains 163 species, and 3280 links with a non-zero
101 probability of interaction. The species list for the Canadian metaweb was extracted from the International Union
102 for the Conservation of Nature (IUCN) checklist (Strydom *et al.* 2022). The metaweb was reconstructed using
103 graph embedding and phylogenetic transfer learning based on the metaweb of European terrestrial mammals,
104 which is itself based on a comprehensive survey of interactions reported in the scientific literature (Maiorano *et*
105 *al.* 2020) – the European metaweb is likely the most extensive collective collection of such interactions
106 available today. The Canadian metaweb showed a 91% success rate in its correct identification of known
107 interactions between Canadian mammals recorded in global databases (Strydom *et al.* 2022). This metaweb is
108 probabilistic, which has the advantage of reflecting the likelihood of an interaction taking place given the
109 phylogenetic and trait match between two species; in other words, the probability of an interaction in the
110 metaweb describes our confidence in the biological feasibility of this interaction. This allows incorporating
111 interaction variability between species (*i.e.*, taking into account that two species may not always interact
112 whenever or wherever they occur); however, other factors beyond trait and phylogenetic matching (*e.g.*,
113 population densities) will also contribute to observed interaction frequencies.

114 **Species occurrences**

115 Downscaling the metaweb involved combining it with species occurrence and environmental data. First, we
116 extracted species occurrences from the Global Biodiversity Information Facility (GBIF; www.gbif.org) for the
117 Canadian mammals after reconciling species names between the Canadian metaweb and GBIF using the GBIF
118 Backbone Taxonomy (GBIF Secretariat 2021). This step removed potential duplicates by combining species
119 listed in the Canadian metaweb which were considered as a single entity by GBIF. We collected occurrences for
120 the updated species list (159 species) using the GBIF download API on October 21st 2022 (GBIF.org 2022).
121 We restricted our query to occurrences with coordinates between longitudes 175°W to 45°W and latitudes 10°N
122 to 90°N. This was meant to collect training data covering a broader range than our prediction target (Canada
123 only) and include observations in similar environments. Then, since GBIF observations represent presence-only
124 data and most predictive models require absence data, we generated the same number of pseudo-absence data as
125 occurrences for every species (Barbet-Massin *et al.* 2012). We weighted candidate sites by their distance to a
126 known observation (separately for each species) using the DistanceToEvent method from the *Julia* package
127 SpeciesDistributionToolkit, making it more likely to select sites further away from an observation and the
128 known species range. This is because our intent was to model the potential distribution of species, capturing
129 wider responses to the environment, as the downscaled metaweb we aimed to produce is potential in nature (see
130 *Downscaled metaweb* section below). We used the Haversine distance between observation and candidate
131 pseudo-absence cells when drawing pseudo-absences.

132 **Environmental data**

133 We used species distribution models (SDMs, Guisan & Thuiller 2005) to project Canadian mammal habitat
134 suitability across the country, which we treated as information on potential distribution. For each species, we
135 related occurrences and pseudo-absences with 19 bioclimatic variables from CHELSA (Karger *et al.* 2017) and
136 12 consensus land-cover variables from EarthEnv (Tuanmu & Jetz 2014). The CHELSA bioclimatic variables
137 (*BIO1-BIO19*) represent various measures of temperature and precipitation (*e.g.*, annual averages, monthly
138 maximum or minimum, seasonality) and are available for land areas across the globe. We used the most recent
139 version, the CHELSA v2.1 dataset (Karger *et al.* 2021), and subsetting it to land surfaces only using the
140 CHELSA v1.2 (Karger *et al.* 2018), which does not cover open water (this is appropriate as the data we use as
141 input only cover terrestrial mammals). The EarthEnv land-cover variables represent classes such as Evergreen

142 broadleaf trees, Cultivated and managed vegetation, Urban/Built-up, and Open Water. Values range between 0
143 and 100 and represent the consensus prevalence of each class in percentage within a pixel (hereafter called a
144 “site”). We coarsened both the CHELSA and EarthEnv data from their original 30 arc-second resolution to a
145 2.5 arc-minute one (around 4.5 km at the Equator) using GDAL (Rouault *et al.* 2024). This resolution
146 compromised capturing both local variations and broad-scale patterns while limiting computation costs to a
147 manageable level as memory requirements rapidly increase with spatial resolution.

148 **Analyses**

149 **Species distribution models**

150 Our selection criteria for choosing an SDM algorithm was to have a method that generated probabilistic results
151 (similar to Gravel *et al.* 2019), including both a probability of occurrence for a species in a specific site and the
152 uncertainty associated with the prediction. These were crucial to obtaining a probabilistic version of the
153 metaweb as they were used to create spatial variations in the localized interaction probabilities (see next
154 section). One suitable method for this is Gradient Boosted Trees with a Gaussian maximum likelihood estimator
155 from the `EvoTrees.jl` Julia package (<https://github.com/Evoest/EvoTrees.jl>). This method returns a
156 prediction for every site with an average value and a standard deviation, which we considered as a measure of
157 uncertainty; specifically, the output of a Gaussian MLL BRT is the probability distribution of observing the
158 positive (*i.e.*, presence) class. We used the mean and standard deviation of the predicted outcome to build a
159 Normal distribution for the probability of occurrence of a given species at each site (represented as probability
160 distributions on Fig. 1). We trained models across the extent chosen for occurrences (longitudes 175°W to 45°W
161 and latitudes 10°N to 90°N), then predicted species distributions only for Canada. We used the 2021 Census
162 Boundary Files from Statistics Canada (Statistics Canada 2022) to set the boundaries for our predictions, which
163 gave us 970,698 sites in total. Performance evaluation for the single species SDMs are available on [GitHub](#).

164 **Building site-level instances of the metaweb**

165 The next part of the workflow was to produce local metawebs for every site (*Localized steps* box on Fig. 1). This
166 component was divided into single-species, two-species, and network-level steps.

167 The single-species steps represented four possible ways to account for uncertainty in the species distributions
168 and bring variation to the spatial metaweb. We explored four different options to select a value ($P(\text{occurrence})$;

Fig. 1) from the occurrence distributions obtained in the previous steps: 1) taking the mean from the distribution as the probability of occurrence (option 1 in Fig. 1); 2) converting the mean value to a binary one using a specific threshold per species (option 2); 3) sampling a random value within the Normal distribution (option 3); or 4) converting a random value into a binary result (option 4, using a separate draw from option 3 and the same threshold as in option 2). The threshold (τ in Fig. 1) used was the value that maximized Youden's J informedness statistic (Youden 1950), the same metric used by Strydom *et al.* (2022) at an intermediate step while building the metaweb. The four sampling options were intended to explore how uncertainty and variation in the species distributions can affect the metaweb result. We expected thresholding to have a more pronounced effect on network structure as it should reduce the number of links by removing many of the rare interactions (Poisot *et al.* 2016). On the other hand, we expected random sampling to create higher spatial heterogeneity compared to the mean probabilities, as including some extreme values should confound the main trends promoted by environmental gradients. We chose option 1 to present our results as it is intuitive and essentially represents the result of a probabilistic SDM (as in Gravel *et al.* 2019), but results obtained with other sampling strategies are available in Supplementary Material.

Next, the two-species steps were aimed at assigning a probability of observing an interaction between two species in a given site. For each species pair, we multiplied the product of the two species' occurrence probabilities ($P(\text{co-occurrence})$; Fig. 1) (obtained using one of the sampling options above) by their interaction probability in the Canadian metaweb. For cases where species in the Canadian metaweb were considered as the same species by the GBIF Backbone Taxonomy (the reconciliation step mentioned earlier), we used the highest interaction probabilities involving the duplicated species.

The network-level steps then created the probabilistic metaweb for the site. We assembled all the local interaction probabilities (from the two-species steps) into a probabilistic network (Poisot *et al.* 2016). We then sampled several random network realizations to represent the potential local realization process (Poisot *et al.* 2015). This resulted in a distribution of localized networks, which we averaged over the number of simulations to obtain a single probabilistic network for the site.

Downscaled metaweb

The final output of our workflow was the downscaled metaweb, which contains a localized probabilistic metaweb in every site across the study area (*Outputs* box in Fig. 1). The metaweb sets an upper bound on the potential interactions (Strydom *et al.* 2023), therefore, the downscaled metaweb is a refined upper boundary at

the local scale that takes into account co-occurrences. It is still potential in nature and differs from a local realization, from which it should have a different structure. Nonetheless, from the downscaled metaweb, we can create maps of network properties (*e.g.*, number of links, connectance) measured on the local probabilities of species interactions and occurrences, and compute some traditional community-level measures such as species richness. We chose to compute and display the expected number of links (measured on probabilistic networks following Poisot *et al.* 2016; see Gravel *et al.* 2019 for a similar example) as its relationship with species richness has been highlighted in a spatial context in recent studies (Galiana *et al.* 2021, 2022). We also computed the uncertainty associated with the community and network measurements (richness variance and link variance, respectively) and compared their spatial distribution (see Supplementary Material).

Analyses of results by ecoregions

Since both species composition and network summary values display a high spatial variation and complex patterns, we simplified the representation of their distribution by grouping sites by ecoregion, as species and interaction composition have been shown to differ between ecoregions across large spatial scales (Martins *et al.* 2022). To do so, we rasterized the Canadian subset of the global map of ecoregions from (Dinerstein *et al.* 2017; also used by Martins *et al.* 2022), which resulted in 44 different ecoregions. For every measure we report (*e.g.*, species richness, number of links), we calculated the median site value for each ecoregion, as a way to avoid bias due to long tails in the distributions. We also measured within-ecoregion variation as the 89% interquantile range of the site values in each ecoregion (threshold chosen to avoid confusion with conventional significance tests; McElreath 2020).

Analyses of ecological uniqueness

We compared the compositional uniqueness of the networks and the communities to assess whether they indicated areas of exceptional composition. We measured uniqueness using the local contributions to beta diversity (LCBD, Legendre & De Cáceres 2013), which identify sites with exceptional composition by quantifying how much one site contributes to the total variance in the community composition. While many studies used LCBD values to evaluate uniqueness on local scales or few study sites (for example, da Silva & Hernández 2014; Heino & Grönroos 2017), recent studies used the measure on predicted species compositions over broad spatial extents and a large number of sites (Dansereau *et al.* 2022; Vasconcelos *et al.* 2018). LCBD

values can also be used to measure uniqueness for networks by computing the values over the adjacency matrix, which has been shown to capture more unique sites and uniqueness variability than through species composition (Poisot *et al.* 2017). Here, we measured and compared the uniqueness of our localized community and network predictions. For species composition, we assembled a site-by-species community matrix (970,698 sites by 159 species) with the probability of occurrence of each species at every site obtained in the species distribution models. For network composition, we assembled a site-by-interaction matrix with the localized probability of interaction at every site given by the downscaled metaweb (therefore, 970,698 sites by 3,108 interactions with defined probabilities in the metaweb). We applied the Hellinger transformation on both matrices and computed the LCBD values from the total variance in the matrices (Legendre & De Cáceres 2013). High LCBD values indicate a high contribution to the overall variance and a unique species or interaction composition compared to other sites. Since the values themselves are very low given our high number of sites (as in Dansereau *et al.* 2022), what matters primarily is the magnitude of the difference between the sites. Given this, we divided values by the maximum value in each matrix (species or network) and suggest that these should be viewed as relative contributions compared to the highest observed contribution. As with other measures, we then summarized the local uniqueness values by ecoregion by taking the median LCBD value and measuring the 89% interquantile range.

Analyses of network motifs

To further explore network structure in space, we investigated the distribution of network motifs across space. Motifs are defined sets of interaction between species (Milo *et al.* 2002; Stouffer *et al.* 2007), for instance two predators sharing one prey, which are repeated within larger and more complex food webs. Motifs are linked to community persistence (Stouffer & Bascompte 2010) and community structure (Cirtwill & Stouffer 2015; Simmons *et al.* 2019), are conserved across scales (Baiser *et al.* 2016; Baker *et al.* 2015), and are part of a common backbone of interactions among all food webs (Mora *et al.* 2018). We focused on four of the most studied three-species motifs (Baiser *et al.* 2016; Stouffer *et al.* 2007; Stouffer & Bascompte 2010): S1 (tri-trophic food chains), S2 (omnivory), S4 (exploitative competition) and S5 (apparent competition). These motifs can be grouped into two pairs according to their ecological information: S1 and S2 highlight different trophic structures, while S4 and S5 indicate different competition types. Therefore, we compared the spatial distribution of the motifs in each pair to see which ones were dominant across all our sites. First, we computed the expected motif count for each of the four motifs for all sites using the localized probabilistic networks from

the downscaled metaweb (following Poisot *et al.* 2016). Then, we compared the expected counts of the motifs within the two pairs. To do so, we used a normalized difference measure similar to the Normalized Difference Vegetation Index (NDVI), where we compute the difference between the two motif counts over their sum. We called the index comparing the two trophic motifs (S1 and S2) the Normalized Difference Trophic Index (NDTI) and the one comparing the competition motifs (S4 and S5) the Normalized Difference Competition Index. We defined both indexes as:

$$NDTI = \frac{(S1 - S2)}{(S1 + S2)}$$

$$NDCI = \frac{(S4 - S5)}{(S4 + S5)}$$

Values for both indexes are bounded between -1 and 1. A value of 0 indicates that both motifs have the same expected counts. Positive values indicate that the first motif in each index (S1 and S4) is dominant and has a higher expected count, while negative values indicate that the second motif (S2 and S5) is dominant. As with previous measures, we then summarized both index values by ecoregion by taking the ecoregion median and measuring its within-ecoregion variation with the 89% interquantile range. Ecoregion values therefore indicate if one type of trophic structure (for NDTI) and one type of competition (for NDCI) is dominant in the ecoregion, while the interquantile range values measure whether the dominant type varies within the ecoregion.

We used *Julia* v1.9.0 (Bezanson *et al.* 2017) to implement all our analyses. We used packages `GBIF.jl` (Dansereau & Poisot 2021) to reconcile species names using the GBIF Backbone Taxonomy, `SpeciesDistributionToolkit.jl` (<https://github.com/PoisotLab/SpeciesDistributionToolkit.jl>) to handle raster layers, species occurrences and generate pseudo-absences (using the `DistanceToEvent` method), `EvoTrees.jl` (<https://github.com/Evoest/EvoTrees.jl>) to perform the Gradient Boosted Trees, `EcologicalNetworks.jl` (Poisot *et al.* 2019) to analyze network and metaweb structure, and `Makie.jl` (Danisch & Krumbiegel 2021) to produce figures. Our data sources (CHELSA, EarthEnv, Ecoregions) were all unprojected, and we did not use a projection in our analyses. However, we displayed the results using a Lambert conformal conic projection more appropriate for Canada using `GeoMakie.jl` (<https://github.com/MakieOrg/GeoMakie.jl>). All the code used to implement our analyses is archived on Zenodo (<https://doi.org/10.5281/zenodo.8350065>; Dansereau & Poisot 2023) and includes instructions on how to run a smaller example at a coarser resolution. Note that running our analyses at full scale is resource and memory-intensive and required the use of computer clusters provided by Calcul Québec and the Digital Research Alliance of Canada. Full-scale computations (excluding motifs) required 900 CPU core-hours and

282 peaked at 500 GB of RAM. Computations for network motifs were substantially more demanding, requiring
283 about 12 CPU core-years (approx. 10^5 hours).

284 Results

285 Our workflow allowed us to display the spatial distribution of ecoregion-level community measures (here,
286 expected species richness) and network measures (expected number of links; Fig. 2). We highlight that the
287 measures presented here are first computed over the predicted communities and networks obtained when
288 downscaling the metaweb, then summarized across the ecoregions (taking the median within each ecoregion).
289 They are not a direct prediction of the measure itself (*e.g.*, we do not present a prediction of actual species
290 richness at each location). Expected ecoregion richness (Fig. 2A) and expected number of links (Fig. 2B)
291 displayed similar distributions with a latitudinal gradient and higher values in the south. Within-ecoregion
292 variability was distributed slightly differently with a less constant latitudinal gradient, notably lower
293 interquartile ranges near the southern border (for example, near Vancouver Island and the Rockies on the West
294 Coast, and near the Ontario Peninsula, the Saint-Lawrence Valley, and Central New-Brunswick in the East;
295 Fig. 2C-D). Bivariate comparison of the distributions of species richness and expected number of links and of
296 their respective within-ecoregion variability further shows some areas of mismatches, indicating that richness
297 and links do not co-vary completely although they may show similar distributions for median values (see
298 Supplementary Material, Fig. S1). All results shown are based on the first sampling strategy (option 1)
299 mentioned in the *Building site-level instances of the metaweb* section, where we used the mean value of the
300 species distributions as the species occurrence probabilities (results for other sampling strategies are shown in
301 Supplementary Material, Fig. S2). Site-level results (before summarizing by ecoregion) are also provided in
302 Supplementary Material (Figs. S3-S6).

303 [Figure 2 about here.]

304 Our results also indicate a mismatch between the uniqueness of communities and networks (Fig. 3). Uniqueness
305 was higher mostly in the north and along the south border for communities, but mainly in the north for networks
306 (Fig. 3A-B). Consequently, ecoregions with both unique community composition and unique network
307 composition were mostly in the north (Fig. 3C). Meanwhile, some areas were unique for one element but not the
308 other. For instance, ecoregions along the south border had a unique species composition but a more common

309 network composition (Fig. 3C). Two ecoregions showed the opposite (unique network compositions only) at
310 higher latitudes (Davis Highlands tundra, near 70°N, and Southern Hudson Bay taiga, near 54°N). Moreover,
311 network uniqueness values for ecoregions spanned a narrower range between the 44 ecoregions than species
312 LCBD values (Fig. 3D, left). Within-ecoregion variation was also lower for network values with generally lower
313 89% interquantile ranges among the site-level LCBD values (Fig. 3D, right).

314 [Figure 3 about here.]

315 Comparing the distribution of dominant network motifs revealed additional areas of variation in network
316 structure (Fig. 4). NDTI displayed a latitudinal gradient between the trophic motifs. Northern ecoregions
317 showed positive NDTI values and high dominance of S1 (tri-trophic chains) expected counts compared to S2
318 (omnivory) but ecoregions along the south border showed a reduced dominance (Fig. 4A). Ecoregions near the
319 Ontario Peninsula and Saint-Lawrence Valley showed values close to zero, indicating a balance between two
320 motifs, while Central New Brunswick had slightly negative values, indicating a low dominance of S2. In
321 comparison, NDCI values showed an evenly high dominance of S5 (apparent competition) over S4 (exploitative
322 competition) across all ecoregions (Fig. 4B). Meanwhile, within-ecoregion variance displayed a different spatial
323 distribution from the median values. NDTI interquantile ranges spanned a wide range of values and were higher
324 both in the north and in the south (although not in the ecoregions with higher NDTI median values) (Fig. 4C).
325 On the other hand, NDCI interquantile ranges showed lower within-ecoregion variance in most ecoregions
326 except in the northernmost one (Canadian High Arctic tundra), which has a notably higher value (Fig. 4D).
327 Although this higher variance does not reflect in the NDCI median values, it does appear when looking at the
328 site-level values, where this ecoregion is the only one with patches with high positive NDCI values (indicating a
329 dominance of S4) surrounded by highly negative values (indicating a dominance of S5) as in other ecoregions
330 (Fig. S6B).

331 [Figure 4 about here.]

332 Discussion

333 Our approach presents a way to downscale a metaweb, produce localized predictions using probabilistic
334 networks as inputs and outputs, and incorporate uncertainty, as called for by Strydom *et al.* (2023). It gives us

an idea of what local metawebs or networks could look like in space, given species distributions and their variability, as well as the uncertainty around species interactions. We also provide the first spatial representation of the metaweb of Canadian mammals (Strydom *et al.* 2022) and a probabilistic equivalent to how the European tetrapod metaweb (Maiorano *et al.* 2020) was used to predict localized networks in Europe (Botella *et al.* 2024; Braga *et al.* 2019; Galiana *et al.* 2021; Gaüzère *et al.* 2022; O'Connor *et al.* 2020). Therefore, our approach could open similar possibilities of investigations on the variation of structure in space (Braga *et al.* 2019) and on the effect of land-use intensification (Botella *et al.* 2024) on North American food webs, particularly Canadian mammal food webs. Other interesting research applications include assessing climate change impacts on network structure (*e.g.*, Kortsch *et al.* 2015) or investigating linkages between network structure and stability (Windsor *et al.* 2023).

As our approach is probabilistic, it does not assume species interact whenever they co-occur and incorporates variability based on environmental conditions (via projected species distributions), which could lead to different results by introducing a different association between species richness and network properties. Galiana *et al.* (2021) found that species richness had a large explanatory power over network properties, but mentioned this could potentially be due to interactions between species being constant across space. Here, we found that potential species richness and number of links displayed similar distributions following a latitudinal gradient, but that the within-ecoregion variance was lower along the southern border than the measures themselves (Fig. 2). The causes for this lack of consistency at the eco-region scale could be verified in future studies; for instance, higher urban density in the south can create more heterogeneity within an eco-region, and the variability in network structure may reflect true landscape variability within eco-regions. We found that network density (links on Fig. 2B) was lower in the north, which is contrary to what was observed in Europe for the terrestrial tetrapod metaweb (Braga *et al.* 2019; Galiana *et al.* 2021) and for willow-galler-parasitoid networks (Gravel *et al.* 2019), where connectance was higher in northern regions. However, those are systems with different numbers of species and environmental conditions (*e.g.*, Europe and Canada could differ due to varying climatic conditions, land-use, and species composition at the same latitudes). Further research should investigate why these results might differ between continents and ecological systems and whether it is due to the methodology, data, or biogeographical processes.

Our LCBD and uniqueness results highlighted that areas with unique network composition differ from sites with unique species composition. In other words, the joint distribution of community and network uniqueness highlights different diversity hotspots. Poisot *et al.* (2017) showed a similar result with host-parasite

communities of rodents and ectoparasitic fleas. Our results further show that these differences could be distributed across ecoregions and over a broad spatial extent for mammal food webs. LCBD scores essentially highlight variability hotspots and are a measure of the variance of community or network structure. Here, they also serve as an inter-ecoregion variation measure, which can be compared to the within-ecoregion variation highlighted by the interquantile ranges. The narrower range of values for network LCBD values and the lower IQR values indicate that both the inter-ecoregion and within-ecoregion variation are lower for networks than for species (Fig. 3).

Our analysis of the distribution of dominant network motifs revealed additional areas of variation in network structure. Trophic motifs (S1 and S2, measured through NDTI values) showed a latitudinal gradient different from the richness and links ones, with high dominance of tri-trophic chains (S1) in the north and higher omnivory counts (S2) only in a few ecoregions in the south. These results did not seem related to ecoregion variance, which once again showed a very different distribution from the median values. Meanwhile, competition motifs (S4 and S5, measured through NDCI values) showed an even dominance of apparent competition (S5) but high variance in a single ecoregion. Overall, our results show that dominant motifs within a mammal food web not only vary between ecoregions, but actually vary differently across space.

When to use the workflow we presented here will depend on the availability of interaction data or existing metawebs, and on the intent to incorporate interaction variability, as well as ecoregion-level variability. In systems where *in situ* interaction and complete network data are available, the approach put forward by Gravel *et al.* (2019) achieves a similar purpose as we attempted here, but is more rigorous and allows modelling the effect of the environment on the interactions themselves. Without such data, establishing or predicting the metaweb (*e.g.*, using transfer learning) should be the first step toward producing localized predictions (Strydom *et al.* 2023). Our framework then downscales the metaweb towards the localized predictions, here using the probabilistic Canadian mammal one, but it can also use other metawebs generated through various means. Well-documented binary ones such as the European tetrapod metaweb could be partly combined with our approach if used with probabilistic SDMs and summarized by ecoregions (as they would only lack an initial probabilistic metaweb, but would still obtain a more probabilistic output). Our approach will essentially differ from previous attempts in how it perceives uncertainty and variability. For instance, rare interactions should not be over-represented (Poisot *et al.* 2016) and should have lesser effects over computed network measures. Furthermore, summarizing results by ecoregion allows for showing variation within and between ecologically meaningful biogeographic boundaries (Martins *et al.* 2022), which, as our results showed, is not constant across

395 space and can help identify contrasting diversity hotspots.

396 Although our approach can generate a wealth of predictions, the next step is quite obviously to work on the
397 validation of these predictions. This step is mandatory if the predictions are to be made actionable.

398 Nevertheless, developing a way to generate these predictions when information is initially scarce, as we present
399 here, is highly important in itself: it establishes a baseline for what the expected measurements will look like,
400 but also (through quantification of variability and uncertainty) provides an estimate of where a more sustained
401 effort is required to adequately document food web structure. For instance, documenting interactions at a single
402 location in an eco-region with high variability of predicted network structure may ultimately be less informative,
403 whereas more homogeneous eco-regions constitute “low-hanging fruits” for validation. Any future sampling of
404 food web structure can be used to (in)validate the predictions: they can be fed into the model to iterate these
405 results again, and by decreasing the uncertainty associated to the interactions, can boost the accuracy of the
406 entire model. There are two external sources of information that can also increase the predictive ability of the
407 model. Because the downscaling relies on SDMs, any additional documentation of species presences can be
408 reflected in the network prediction. Furthermore, because the metaweb itself was obtained through transfer
409 learning from data describing a different system, any change to the knowledge in this other data can be reflected
410 in the input data. As Strydom *et al.* (2023) point out, validation of metaweb predictions, empirical sampling,
411 and method design should all proceed jointly, and making conceptual progress in one of these areas helps all the
412 others. In this manuscript, we focused on motif composition, both for its relevance to functional properties of
413 food webs, but also because it can be fairly reliably inferred from partial network data; in other words, validating
414 some predictions is not necessarily relying upon exhaustive documentation of local food webs.

415 The recent shift in focus towards building metawebs opens many opportunities for projections of networks in
416 space through probabilistic downscaling, as we suggested here. Metawebs have been documented in many
417 systems, allowing us to build new ones from predictions. How the European tetrapod metaweb (Maiorano *et al.*
418 2020) was used to predict the Canadian mammal metaweb (Strydom *et al.* 2022) is one such case, but recent
419 examples also extend to other systems. Metawebs have been compiled for many marine food webs (*e.g.*, Barents
420 Sea, Kortsch *et al.* 2019; North Scotia Sea, López-López *et al.* 2022; Gulf of Riga, Kortsch *et al.* 2021) and
421 used to predict the probability of novel interactions (Arctic food web of the Barents sea, Pecuchet *et al.* 2020).
422 Olivier *et al.* (2019) built a temporally resolved metaweb of demersal fish and benthic epifauna but also
423 suggested combining their approach with techniques estimating the probability of occurrence of trophic
424 relationships to describe spatial and temporal variability more accurately. Lurgi *et al.* (2020) built a metaweb

425 and probabilistic (occurrence-based) networks for rocky intertidal communities (and in doing so, they also
426 showed that environmental factors do not affect the structure of binary and probabilistic networks in different
427 ways). Albouy *et al.* (2019) predicted the global marine fish food web using a probabilistic model, showing the
428 potential to describe networks across broad spatial scales. Similarly, predictive approaches are also increasingly
429 used with other interaction types to highlight interaction hotspots on global scales (*e.g.*, mapping geographical
430 hotspots of predicted host-virus interactions between bats and betacoronaviruses, Becker *et al.* 2022; predicting
431 the distribution of hidden interactions in the mammalian virome, Poisot *et al.* 2023). Our workflow offers the
432 potential to bring these global predictions down to the local scale where they can be made more actionable, and
433 vastly increases the diversity of ecological networks that can be projected in space.

434 **Acknowledgements**

435 We acknowledge that this study was conducted on land within the traditional unceded territory of the Saint
436 Lawrence Iroquoian, Anishinabewaki, Mohawk, Huron-Wendat, and Omàmiwininiwak nations. GD is funded
437 by the NSERC Postgraduate Scholarship – Doctoral (grant ES D – 558643), the FRQNT doctoral scholarship
438 (grant no. 301750), and the NSERC CREATE BIOS² program. TP is funded by the Wellcome Trust
439 (223764/Z/21/Z), NSERC through the Discovery Grant and Discovery Accelerator Supplements programs, and
440 the Courtois Foundation. This research was enabled in part by support provided by Calcul Québec
441 (calculquebec.ca) and the Digital Research Alliance of Canada (alliancecan.ca) through the Narval general
442 purpose cluster.

References

- Albouy, C., Archambault, P., Appeltans, W., Araújo, M.B., Beauchesne, D., Cazelles, K., *et al.* (2019). [The marine fish food web is globally connected](#). *Nature Ecology & Evolution*, 3, 1153–1161.
- Baiser, B., Elheshha, R. & Kahveci, T. (2016). [Motifs in the assembly of food web networks](#). *Oikos*, 125, 480–491.
- Baiser, B., Gravel, D., Cirtwill, A.R., Dunne, J.A., Fahimipour, A.K., Gilarranz, L.J., *et al.* (2019). [Ecogeographical rules and the macroecology of food webs](#). *Global Ecology and Biogeography*, geb.12925.
- Baker, N.J., Kaartinen, R., Roslin, T. & Stouffer, D.B. (2015). [Species' roles in food webs show fidelity across a highly variable oak forest](#). *Ecography*, 38, 130–139.
- Barbet-Massin, M., Jiguet, F., Albert, C.H. & Thuiller, W. (2012). [Selecting pseudo-absences for species distribution models: How, where and how many?](#) *Methods in Ecology and Evolution*, 3, 327–338.
- Becker, D.J., Albery, G.F., Sjödin, A.R., Poisot, T., Bergner, L.M., Chen, B., *et al.* (2022). [Optimising predictive models to prioritise viral discovery in zoonotic reservoirs](#). *The Lancet Microbe*, 3, e625–e637.
- Bezanson, J., Edelman, A., Karpinski, S. & Shah, V.B. (2017). [Julia: A fresh approach to numerical computing](#). *SIAM Review*, 59, 65–98.
- Botella, C., Gaüzère, P., O'Connor, L., Ohlmann, M., Renaud, J., Dou, Y., *et al.* (2024). [Land-use intensity influences European tetrapod food webs](#). *Global Change Biology*, 30, e17167.
- Braga, J., Pollock, L.J., Barros, C., Galiana, N., Montoya, J.M., Gravel, D., *et al.* (2019). [Spatial analyses of multi-trophic terrestrial vertebrate assemblages in Europe](#). *Global Ecology and Biogeography*, 28, 1636–1648.
- Cirtwill, A.R. & Stouffer, D.B. (2015). [Concomitant predation on parasites is highly variable but constrains the ways in which parasites contribute to food web structure](#). *Journal of Animal Ecology*, 84, 734–744.
- da Silva, P.G. & Hernández, M.I.M. (2014). [Local and regional effects on community structure of dung beetles in a mainland-island scenario](#). *PLOS ONE*, 9, e111883.
- Danisch, S. & Krumbiegel, J. (2021). [Makie.jl: Flexible high-performance data visualization for Julia](#). *Journal of Open Source Software*, 6, 3349.

469 Dansereau, G., Legendre, P. & Poisot, T. (2022). [Evaluating ecological uniqueness over broad spatial extents](#)
 470 [using species distribution modelling](#). *Oikos*, 2022, e09063.

471 Dansereau, G. & Poisot, T. (2021). [SimpleSDMLayers.jl and GBIF.jl: A framework for species distribution](#)
 472 [modeling in Julia](#). *Journal of Open Source Software*, 6, 2872.

473 Dansereau, G. & Poisot, T. (2023). [PoisotLab/SpatialProbabilisticMetaweb: V1.0](#).

474 Desjardins-Proulx, P., Laigle, I., Poisot, T. & Gravel, D. (2017). [Ecological interactions and the Netflix](#)
 475 [problem](#). *PeerJ*, 5, e3644.

476 Dinerstein, E., Olson, D., Joshi, A., Vynne, C., Burgess, N.D., Wikramanayake, E., *et al.* (2017). [An](#)
 477 [Ecoregion-Based Approach to Protecting Half the Terrestrial Realm](#). *BioScience*, 67, 534–545.

478 Dunne, J. (2006). The network structure of food webs. In: *Ecological Networks: Linking Structure to Dynamics*
 479 *in Food Webs* (eds. Pascual, M. & Dunne, J.). Oxford University Press, Oxford ; New York, pp. 27–86.

480 Frelat, R., Kortsch, S., Kröncke, I., Neumann, H., Nordström, M.C., Olivier, P.E.N., *et al.* (2022). [Food web](#)
 481 [structure and community composition: A comparison across space and time in the North Sea](#). *Ecography*,
 482 2022.

483 Galiana, N., Barros, C., Braga, J., Ficetola, G.F., Maiorano, L., Thuiller, W., *et al.* (2021). [The spatial scaling of](#)
 484 [food web structure across European biogeographical regions](#). *Ecography*, 44, 653–664.

485 Galiana, N., Lurgi, M., Bastazini, V.A.G., Bosch, J., Cagnolo, L., Cazelles, K., *et al.* (2022). [Ecological](#)
 486 [network complexity scales with area](#). *Nature Ecology & Evolution*, 1–8.

487 Gaüzère, P., O'Connor, L., Botella, C., Poggiato, G., Münkemüller, T., Pollock, L.J., *et al.* (2022). [The diversity](#)
 488 [of biotic interactions complements functional and phylogenetic facets of biodiversity](#). *Current Biology*.

489 GBIF Secretariat. (2021). [GBIF Backbone Taxonomy](#).

490 GBIF.org. (2022). [GBIF occurrence download](#).

491 Gravel, D., Baiser, B., Dunne, J.A., Kopelke, J.-P., Martinez, N.D., Nyman, T., *et al.* (2019). [Bringing Elton](#)
 492 [and Grinnell together: A quantitative framework to represent the biogeography of ecological interaction](#)
 493 [networks](#). *Ecography*, 42, 401–415.

494 Guisan, A. & Thuiller, W. (2005). [Predicting species distribution: Offering more than simple habitat models](#).
 495 *Ecology Letters*, 8, 993–1009.

496 Heino, J. & Grönroos, M. (2017). [Exploring species and site contributions to beta diversity in stream insect](#)
497 [assemblages](#). *Oecologia*, 183, 151–160.

498 Hortal, J., de Bello, F., Diniz-Filho, J.A.F., Lewinsohn, T.M., Lobo, J.M. & Ladle, R.J. (2015). [Seven Shortfalls](#)
499 [that Beset Large-Scale Knowledge of Biodiversity](#). *Annual Review of Ecology, Evolution, and Systematics*,
500 46, 523–549.

501 Jordano, P. (2016). [Sampling networks of ecological interactions](#). *Functional Ecology*, 30, 1883–1893.

502 Karger, D.N., Conrad, O., Böhner, J., Kawohl, T., Kreft, H., Soria-Auza, R.W., *et al.* (2017). [Climatologies at](#)
503 [high resolution for the earth's land surface areas](#). *Scientific Data*, 4, 170122.

504 Karger, D.N., Conrad, O., Böhner, J., Kawohl, T., Kreft, H., Soria-Auza, R.W., *et al.* (2018). [Data from:](#)
505 [Climatologies at high resolution for the earth's land surface areas](#).

506 Karger, D.N., Conrad, O., Böhner, J., Kawohl, T., Kreft, H., Soria-Auza, R.W., *et al.* (2021). [Climatologies at](#)
507 [high resolution for the earth's land surface areas](#).

508 Kortsch, S., Frelat, R., Pecuchet, L., Olivier, P., Putnis, I., Bonsdorff, E., *et al.* (2021). [Disentangling temporal](#)
509 [food web dynamics facilitates understanding of ecosystem functioning](#). *Journal of Animal Ecology*, 90,
510 1205–1216.

511 Kortsch, S., Primicerio, R., Aschan, M., Lind, S., Dolgov, A.V. & Planque, B. (2019). [Food-web structure](#)
512 [varies along environmental gradients in a high-latitude marine ecosystem](#). *Ecography*, 42, 295–308.

513 Kortsch, S., Primicerio, R., Fossheim, M., Dolgov, A.V. & Aschan, M. (2015). [Climate change alters the](#)
514 [structure of arctic marine food webs due to poleward shifts of boreal generalists](#). *Proceedings of the Royal*
515 *Society B: Biological Sciences*, 282, 20151546.

516 Legendre, P. & De Cáceres, M. (2013). [Beta diversity as the variance of community data: Dissimilarity](#)
517 [coefficients and partitioning](#). *Ecology Letters*, 16, 951–963.

518 López-López, L., Genner, M.J., Tarling, G.A., Saunders, R.A. & O’Gorman, E.J. (2022). [Ecological Networks](#)
519 [in the Scotia Sea: Structural Changes Across Latitude and Depth](#). *Ecosystems*, 25, 457–470.

520 Lucas, P., Thuiller, W., Talluto, M., Polaina, E., Albrecht, J., Selva, N., *et al.* (2023). [Including biotic](#)
521 [interactions in species distribution models improves the understanding of species niche: A case of study](#)
522 [with the brown bear in Europe](#).

523 Lurgi, M., Galiana, N., Broitman, B.R., Kéfi, S., Wieters, E.A. & Navarrete, S.A. (2020). [Geographical](#)
524 [variation of multiplex ecological networks in marine intertidal communities](#). *Ecology*, 101, e03165.

525 Maiorano, L., Montemaggiore, A., Ficetola, G.F., O'Connor, L. & Thuiller, W. (2020). [TETRA-EU 1.0: A](#)
526 [species-level trophic metaweb of European tetrapods](#). *Global Ecology and Biogeography*, 29, 1452–1457.

527 Martins, L.P., Stouffer, D.B., Blendinger, P.G., Böhning-Gaese, K., Buitrón-Jurado, G., Correia, M., *et al.*
528 (2022). [Global and regional ecological boundaries explain abrupt spatial discontinuities in avian frugivory](#)
529 [interactions](#). *Nature Communications*, 13, 6943.

530 McElreath, R. (2020). *Statistical rethinking: A bayesian course with examples in R and Stan*. 2nd edn.
531 Chapman and Hall/CRC, New York.

532 McLeod, A., Leroux, S.J., Gravel, D., Chu, C., Cirtwill, A.R., Fortin, M.-J., *et al.* (2021). [Sampling and](#)
533 [asymptotic network properties of spatial multi-trophic networks](#). *Oikos*, 130, 2250–2259.

534 Mestre, F., Gravel, D., García-Callejas, D., Pinto-Cruz, C., Matias, M.G. & Araújo, M.B. (2022). [Disentangling](#)
535 [food-web environment relationships: A review with guidelines](#). *Basic and Applied Ecology*, 61, 102–115.

536 Milo, R., Shen-Orr, S., Itzkovitz, S., Kashtan, N., Chklovskii, D. & Alon, U. (2002). [Network Motifs: Simple](#)
537 [Building Blocks of Complex Networks](#). *Science*, 298, 824–827.

538 Moens, M., Biesmeijer, J., Huang, E., Vereecken, N. & Marshall, L. (2022). [The importance of biotic](#)
539 [interactions in distribution models depends on the type of ecological relations, spatial scale and range](#).

540 Mora, B.B., Gravel, D., Gilarranz, L.J., Poisot, T. & Stouffer, D.B. (2018). [Identifying a common backbone of](#)
541 [interactions underlying food webs from different ecosystems](#). *Nature Communications*, 9, 2603.

542 Morales-Castilla, I., Matias, M.G., Gravel, D. & Araújo, M.B. (2015). [Inferring biotic interactions from](#)
543 [proxies](#). *Trends in Ecology & Evolution*, 30, 347–356.

544 O'Connor, L.M.J., Pollock, L.J., Braga, J., Ficetola, G.F., Maiorano, L., Martinez-Almoyna, C., *et al.* (2020).
545 [Unveiling the food webs of tetrapods across Europe through the prism of the Eltonian niche](#). *Journal of*
546 *Biogeography*, 47, 181–192.

547 Olivier, P., Frelat, R., Bonsdorff, E., Kortsch, S., Kröncke, I., Möllmann, C., *et al.* (2019). [Exploring the](#)
548 [temporal variability of a food web using long-term biomonitoring data](#). *Ecography*, 42, 2107–2121.

549 Pecuchet, L., Blanchet, M.-A., Frainer, A., Husson, B., Jørgensen, L.L., Kortsch, S., *et al.* (2020). [Novel](#)
550 [feeding interactions amplify the impact of species redistribution on an Arctic food web](#). *Global Change*

551 *Biology*, 26, 4894–4906.

552 Poggiato, G., Andréoletti, J., Shirley, L. & Thuiller, W. (2022). [Integrating food webs in species distribution](#)
553 [models improves ecological niche estimation and predictions](#) (Preprint). Authorea.

554 Poisot, T., Bélisle, Z., Hoebeke, L., Stock, M. & Szefer, P. (2019). [EcologicalNetworks.jl: Analysing ecological](#)
555 [networks of species interactions](#). *Ecography*, 42, 1850–1861.

556 Poisot, T., Bergeron, G., Cazelles, K., Dallas, T., Gravel, D., MacDonald, A., *et al.* (2021). [Global knowledge](#)
557 [gaps in species interaction networks data](#). *Journal of Biogeography*, 48, 1552–1563.

558 Poisot, T., Canard, E., Mouillot, D., Mouquet, N. & Gravel, D. (2012). [The dissimilarity of species interaction](#)
559 [networks](#). *Ecology Letters*, 15, 1353–1361.

560 Poisot, T., Cirtwill, A.R., Cazelles, K., Gravel, D., Fortin, M.-J. & Stouffer, D.B. (2016). [The structure of](#)
561 [probabilistic networks](#). *Methods in Ecology and Evolution*, 7, 303–312.

562 Poisot, T., Guéveneux-Julien, C., Fortin, M.-J., Gravel, D. & Legendre, P. (2017). [Hosts, parasites and their](#)
563 [interactions respond to different climatic variables](#). *Global Ecology and Biogeography*, 26, 942–951.

564 Poisot, T., Ouellet, M.-A., Mollentze, N., Farrell, M.J., Becker, D.J., Brierley, L., *et al.* (2023). [Network](#)
565 [embedding unveils the hidden interactions in the mammalian virome](#). *Patterns*, 4, 100738.

566 Poisot, T., Stouffer, D.B. & Gravel, D. (2015). [Beyond species: Why ecological interaction networks vary](#)
567 [through space and time](#). *Oikos*, 124, 243–251.

568 Rouault, E., Warmerdam, F., Schwehr, K., Kiselev, A., Butler, H., Łoskot, M., *et al.* (2024). [GDAL](#).

569 Saravia, L.A., Marina, T.I., Kristensen, N.P., De Troch, M. & Momo, F.R. (2022). [Ecological network](#)
570 [assembly: How the regional metaweb influences local food webs](#). *Journal of Animal Ecology*, 91, 630–642.

571 Simmons, B.I., Cirtwill, A.R., Baker, N.J., Wauchope, H.S., Dicks, L.V., Stouffer, D.B., *et al.* (2019). [Motifs in](#)
572 [bipartite ecological networks: Uncovering indirect interactions](#). *Oikos*, 128, 154–170.

573 Statistics Canada. (2022). *Boundary files, reference guide second edition, Census year 2021*. Second edition.

574 Statistics Canada = Statistique Canada, Ottawa.

575 Stouffer, D.B. & Bascompte, J. (2010). [Understanding food-web persistence from local to global scales](#).
576 *Ecology Letters*, 13, 154–161.

577 Stouffer, D.B., Camacho, J., Jiang, W. & Nunes Amaral, L.A. (2007). [Evidence for the existence of a robust](#)
578 [pattern of prey selection in food webs](#). *Proceedings of the Royal Society B: Biological Sciences*, 274,
579 1931–1940.

580 Strydom, T., Bouskila, S., Banville, F., Barros, C., Caron, D., Farrell, M.J., *et al.* (2022). [Food web](#)
581 [reconstruction through phylogenetic transfer of low-rank network representation](#). *Methods in Ecology and*
582 *Evolution*, 13, 2838–2849.

583 Strydom, T., Bouskila, S., Banville, F., Barros, C., Caron, D., Farrell, M.J., *et al.* (2023). [Graph embedding and](#)
584 [transfer learning can help predict potential species interaction networks despite data limitations](#). *Methods in*
585 *Ecology and Evolution*, 14, 2917–2930.

586 Strydom, T., Catchen, M.D., Banville, F., Caron, D., Dansereau, G., Desjardins-Proulx, P., *et al.* (2021). [A](#)
587 [roadmap towards predicting species interaction networks \(across space and time\)](#). *Philosophical*
588 *Transactions of the Royal Society B: Biological Sciences*, 376, 20210063.

589 Tuanmu, M.-N. & Jetz, W. (2014). [A global 1-km consensus land-cover product for biodiversity and ecosystem](#)
590 [modelling](#). *Global Ecology and Biogeography*, 23, 1031–1045.

591 Vasconcelos, T.S., Nascimento, B.T.M. do & Prado, V.H.M. (2018). [Expected impacts of climate change](#)
592 [threaten the anuran diversity in the Brazilian hotspots](#). *Ecology and Evolution*, 8, 7894–7906.

593 Windsor, F.M., van den Hoogen, J., Crowther, T.W. & Evans, D.M. (2023). [Using ecological networks to](#)
594 [answer questions in global biogeography and ecology](#). *Journal of Biogeography*, 50, 57–69.

595 Wisz, M.S., Pottier, J., Kissling, W.D., Pellissier, L., Lenoir, J., Damgaard, C.F., *et al.* (2013). [The role of biotic](#)
596 [interactions in shaping distributions and realised assemblages of species: Implications for species](#)
597 [distribution modelling](#). *Biological Reviews*, 88, 15–30.

598 Youden, W.J. (1950). [Index for rating diagnostic tests](#). *Cancer*, 3, 32–35.

599 Zarnetske, P.L., Baiser, B., Strecker, A., Record, S., Belmaker, J. & Tuanmu, M.-N. (2017). [The Interplay](#)
600 [Between Landscape Structure and Biotic Interactions](#). *Current Landscape Ecology Reports*, 2, 12–29.

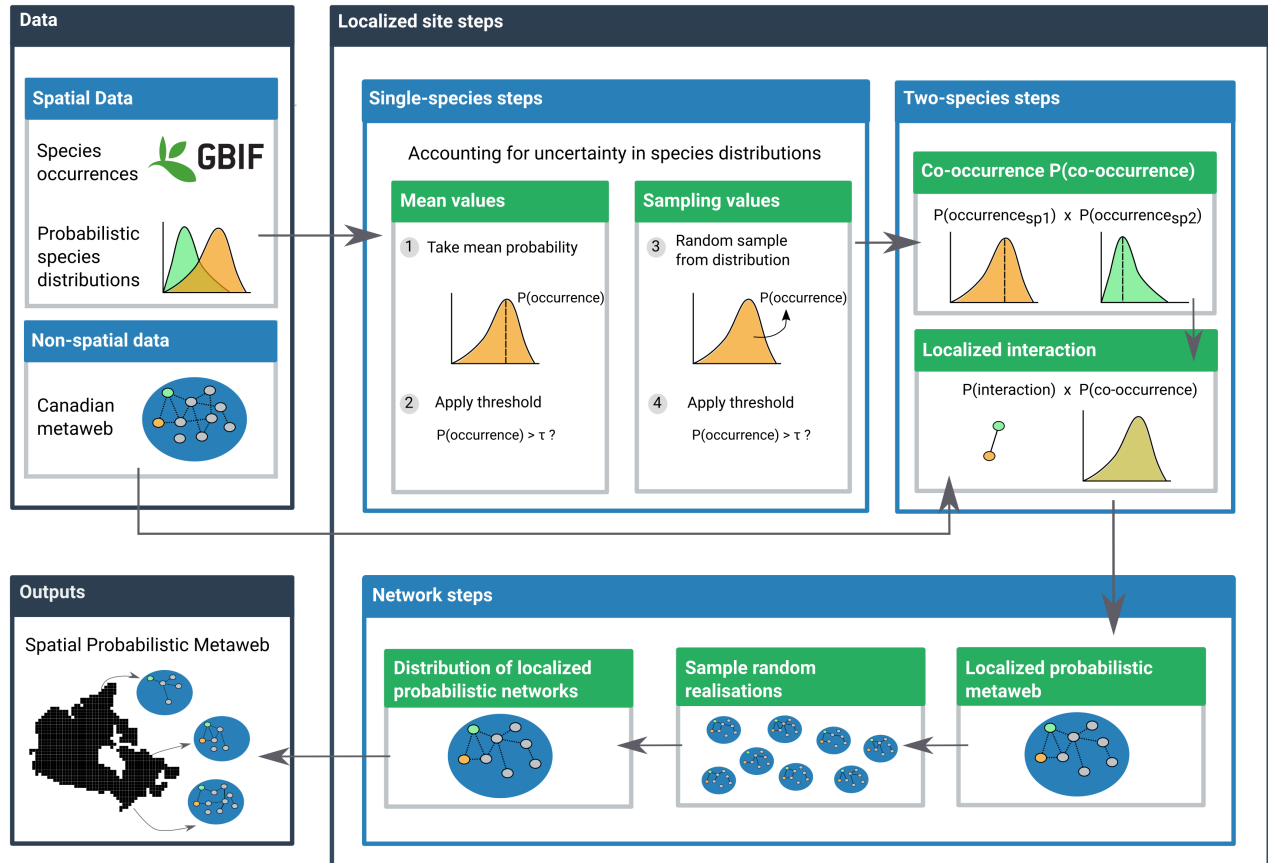


Figure 1: Conceptual figure of the proposed workflow used to downscale the probabilistic metaweb in space. The workflow has three components: the data, the localized steps, and the final spatial output. The data are composed of spatial data (with information in every cell) and non-spatial data (constant for all of Canada). The localized steps use these data and are performed separately in every cell, first at a single-species level (using distribution data), then for every species pair (adding interaction data from the metaweb), and finally at the network level by combining the results of all species pairs. The final output of the network-level steps contains a downscaled probabilistic metaweb for every cell across the study extent. Note that in order to mitigate some of the fine-scale grain in the data, we present most outputs at the ecoregion scale, with pixel-scale maps in supplementary material.

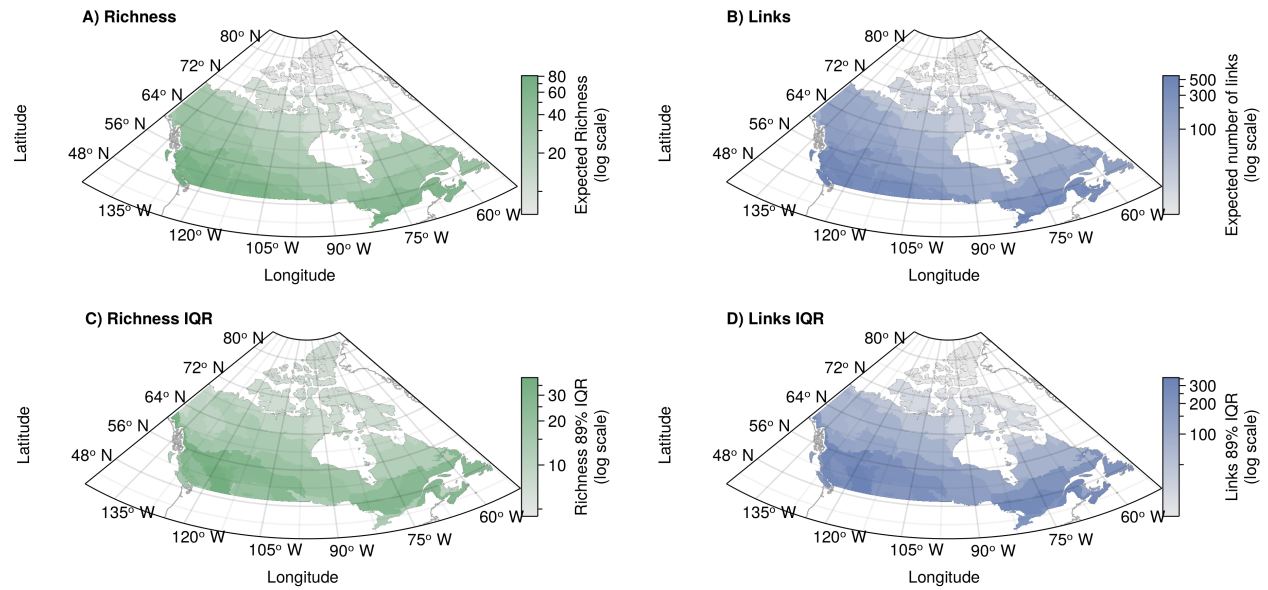


Figure 2: (A-B) Example of a community measure (A, expected species richness) and a network one (B, expected number of links). Both measures are assembled from the predicted probabilistic communities and networks, respectively. Values are first measured separately for all sites; then, the median value within each ecoregion was taken to represent the ecoregion-level value. (C-D) Representation of the 89% interquantile range of values within the ecoregion for expected richness (C) and expected number of links (D). All colour bars follow a log scale with tick marks representing even intervals. Real values (non-log transformed) are shown beside major tick marks while minor ticks represent half increments.

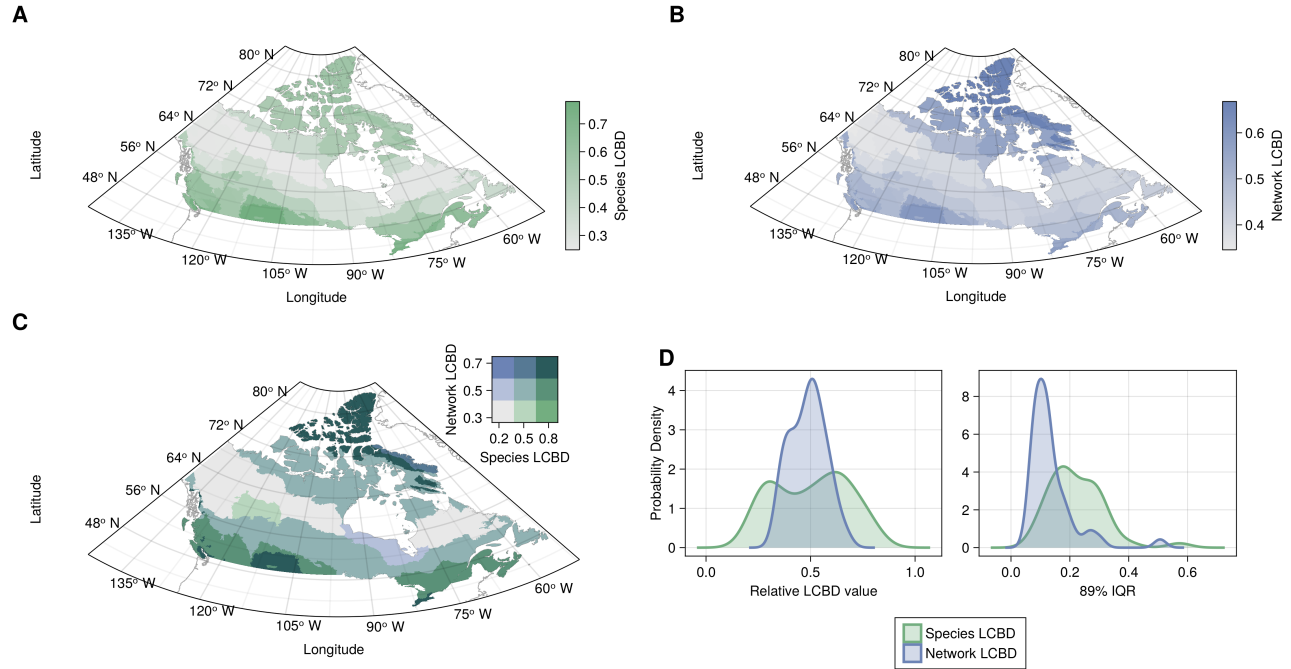


Figure 3: (A-B) Representation of the ecoregion uniqueness values based on species composition (A) and network composition (B). LCBD values were first computed across all sites and scaled relative to the maximum value observed. The ecoregion LCBD value is the median value for the sites in the ecoregion. (C) Bivariate representation of species and network composition LCBD. Values are grouped into three quantiles separately for each variable. The colour combinations represent the nine possible combinations of quantiles. The species uniqueness (horizontal axis) goes left to right from low uniqueness (light grey, bottom left) to high uniqueness (green, bottom right). The network composition uniqueness goes bottom-up from low uniqueness (light grey, bottom left) to high uniqueness (blue, top left). (D) Probability densities for the ecoregion LCBD values for species and network LCBD (left), highlighting the variability of LCBD values between ecoregions, and the 89% interquartile range of the values within each ecoregion (right), highlighting the variability within the ecoregions.

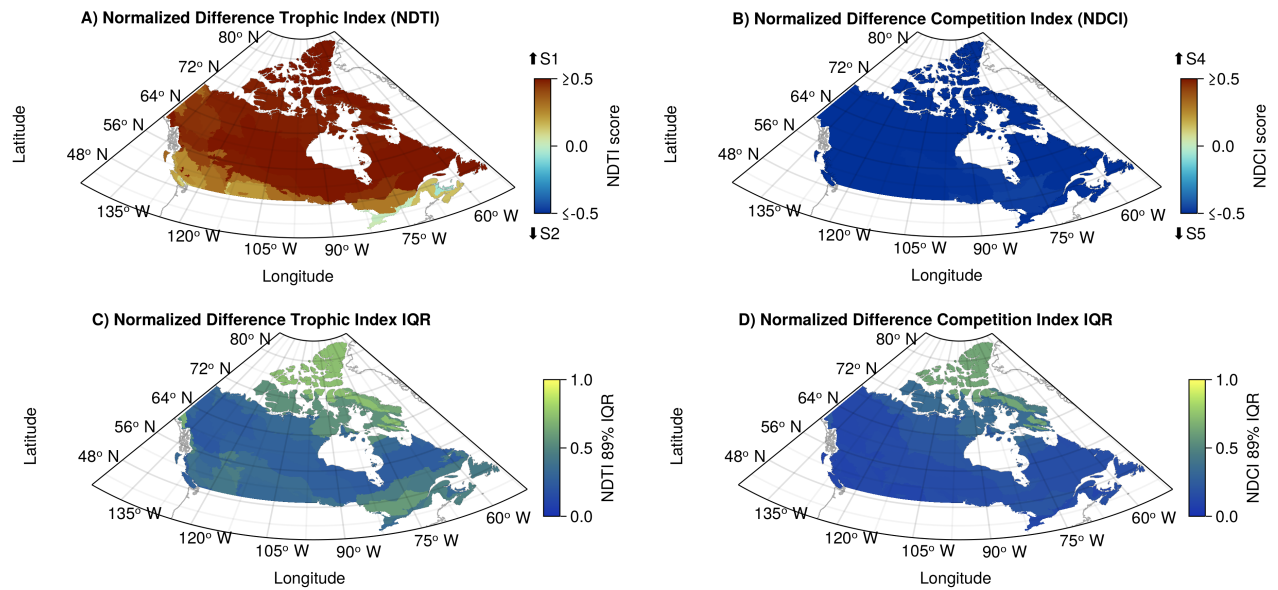


Figure 4: Comparison of the dominant ecological motifs across ecoregions. A) Normalized Difference Index (NDTI) comparing the trophic motifs S1 (tri-trophic food chains) and S2 (omnivory). Positive values indicate a dominance of S1, while negative values indicate a dominance of S2. Values equal or superior to $|0.5|$ are shown with the same colour as they indicate a high dominance of one motif. B) Normalized Difference Index (NDCI) comparing the competition motifs S4 (exploitative competition) and S5 (apparent competition). Positive values indicate a dominance of S4, while negative values indicate a dominance of S5. (C-D) Representation of the 89% interquartile range of values within the ecoregion for the trophic motifs index (NDTI, C) and competition motifs index (NDCI, D).